All-silicon integrated Fabry–Pérot cavity for volume refractive index measurement in microfluidic systems

R. St-Gelais,[a] J. Masson, and Y.-A. Peter[b]
Department of Engineering Physics, Ecole Polytechnique de Montréal, P.O. Box 6079, Station Centre-Ville, Montréal, Quebec H3C 3A7, Canada

(Received 10 March 2009; accepted 18 May 2009; published online 16 June 2009)

We report a refractive index (RI) sensor based on the use of vertically etched silicon Bragg reflectors. The device is robust and performs measurements through tens of micrometers of liquid. A sensitivity of 907 nm/RIU (RI units) and a resolution of 1.7×10^{-5} RIU are obtained and are in good agreement with optical simulations. This resolution is the highest reported for a volume RI sensor integrated with a microfluidic system. Expected applications for the sensor in the fields of single cell characterization and chip based liquid chromatography are discussed. © *2009 American Institute of Physics*. [DOI: 10.1063/1.3152286]

Vertically etched silicon Bragg reflectors have been reported recently to create extrinsic tunable Fabry–Pérot filters for optical fibers. The optical path length between two silicon Bragg reflectors has been tuned using the thermooptic effect,[1] the electro-optic effect,[2] or electrostatic actuation[3–6] in order to vary the resonance wavelength of a Fabry–Pérot filter. In this letter, we report monolithic integration of a similar silicon Fabry–Pérot resonator to a microfluidic system. In this configuration, the optical path length between the two Bragg mirrors is directly related to the refractive index (RI) of the liquid flowing in the microchannel.

RI measurement in microfluidic systems is of great interest since it is label-free and allows detection of the presence or the nature of liquids and biological samples. In order to compare the numerous available technologies, one should make a clear distinction between surface RI and volume RI measurement. Surface RI sensors are based on the interaction between a sample and an evanescent electromagnetic wave. Surface plasmon, integrated dielectric waveguides, and resonant optical microcavities are important example of this type of sensors. Their resolution can be very high [$\sim10^{-7}$ RIU for Ref. 7 (RIU denotes RI units)] but the depth of interaction with the sample is typically small (less than 1 μm). This makes them sensitive to surface contamination and unsuitable for applications requiring thick surface functionalization or measurements through bigger biological samples, such as living cells.

Volume RI sensors for microfluidic systems are based on the beam deviation technique,[8] on laser cavities[9] or, as for the sensor presented in Fig. 1, on Fabry–Pérot cavities. In each case, the light propagates through the sample and the depth of interaction is greatly increased. Other microfluidic Fabry–Pérot refractometers were previously reported[10–13] but they have never been made of silicon/air Bragg reflectors fabricated simultaneously with the microfluidic system. This configuration permits a great flexibility in the design of the microfluidic system, minimizes the number of fabrication steps, and allows to reach the highest resolution reported for a volume RI sensor integrated with a microfluidic system.

Figure 1 presents a schematic view (a) and scanning electron microscope (SEM) photographs [(b) and (c)] of the Fabry–Pérot refractometer integrated with microfluidic elements and optical fiber alignment grooves. The structure is defined by a single photolithography step (SPR220 3.0 photoresist). The silicon is then etched by deep reactive ion etching (DRIE). High verticality and low surface roughness on the optical surfaces (see a detailed discussion on the effect of these imperfections later in the article) are ensured by optimization of the Bosch process, as previously reported.[5] The etch depth is 63 μm in the narrow air layers of the Bragg reflectors and slightly more (80 μm) in the larger openings. This allows insertion of 125 μm diameter conventional SMF-28 single mode optical fibers in the alignment grooves.

Each of the Bragg reflectors is made of three layers of silicon and two layers of air that ensure a high reflectivity[5] because of the large RI contrast ($\Delta n\approx2.45$). The photomask is designed with 2.6 and 1.7 μm thick walls for silicon and

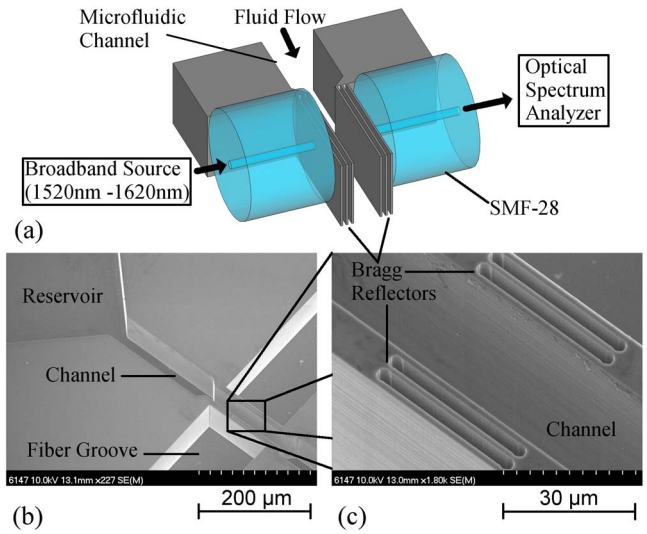

FIG. 1. (Color online) (a) Schematic view of the refractometer connected to the measurement setup through SMF-28 single mode optical fibers. (b) SEM photograph of the Fabry–Pérot refractometer integrated with optical fiber alignment grooves, microfuidic channel, and reservoir. (c) Closeup view of the Fabry–Pérot refractometer made of two silicon/air Bragg reflectors separated by the microfluidic channel.

[a]Electronic mail: raphael.st-gelais@polymtl.ca.
[b]Electronic mail: yves-alain.peter@polymtl.ca. URL: http://www.polymtl.ca/mems.

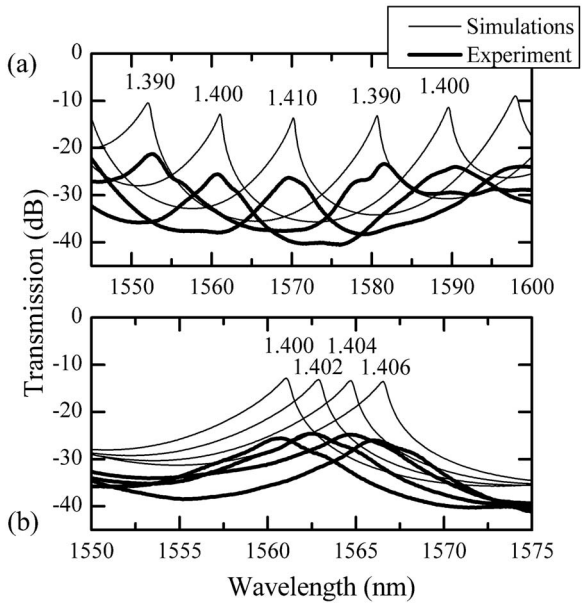

FIG. 2. Measured (thick lines) and simulated (thin lines) transmission spectrum of the Fabry–Pérot refractometer. Curves are labeled by the RI of the liquid filling the channel. (a) Variation of the RI by $\Delta n=0.010$. (b) Variation of the RI by $\Delta n=0.002$.

air, respectively. These dimensions are a compromise between thinner layers, which yield a broader reflection spectrum, and thicker layers, which simplify the fabrication process. With these dimensions, and considering a typical 300 nm undercut of silicon during DRIE, the mirrors have a theoretical reflection bandwidth ($R>90\%$) of 80 nm (see Ref. 5 for more details on the effect of walls thickness on the reflection bandwidth). The length of the cavity (24.5 μm) is chosen to be larger than the thickness of the mirrors (11.1 μm). That way, most of the electromagnetic field of the resonant optical mode is located in the liquid rather than in the mirrors, thus improving the sensitivity.[7]

Measurements are performed at room temperature (~21 °C) with certified RI liquids (Cargille Laboratories, series AA) of low temperature dependence (0.0004 $°C^{-1}$). Liquids placed in the reservoir flow in the microchannel by capillary effect and reach the Fabry–Pérot cavity formed by the two Bragg reflectors. Light from a broadband light source (1520–1620 nm) is incident on the Fabry–Pérot through one of the optical fibers placed in the alignment grooves [see Fig. 1(a)]. The transmitted light is collected by the second optical fiber, which is connected to an Agilent 86142A optical spectrum analyzer.

The experimental and simulated transmission spectrum of the Fabry–Pérot refractometer are presented in Fig. 2. The simulations are based on the transfer matrix method for multilayered optical systems, combined with the Gaussian approximation of the optical fiber fundamental mode, as proposed in Ref. 4. The dimensions of the walls are measured in top view with a SEM, showing an increase of about 1.1 μm of the thickness of the air layers caused by diffraction during photolithography. This is taken into account in the simulations, as well as the typical 300 nm undercut of silicon at each interface during DRIE. These values are then slightly adjusted to 1.086 μm and 312 nm, respectively, to fit with the experimental results.

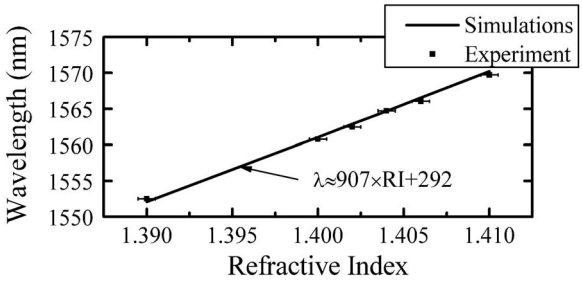

FIG. 3. Simulated and experimental wavelength at maximal transmission between 1550 and 1570 nm, as a function of RI. The error bars represent the uncertainty on the RI of the liquids (±0.0005 around $\lambda=1550$ nm).

As can be seen in Fig. 2, the position and the lineshape of the measured transmission peaks for each RI are in good agreement with the optical simulations. There are however additional losses that are not taken into account by the model. The two possible causes for these losses are scattering by surface roughness and imperfect parallelism between the optical planes. Surface roughness was previously measured by atomic force microscope on the sidewalls of large trenches for devices fabricated using a similar fabrication process.[5] The measured value, $\sigma=26.2$ nm rms, was mainly a result of the periodic scalloping effect caused by the DRIE process. The spatial period of the scalloping ($T=10$ nm) is small compared to the wavelength of light (λ) and satisfies the relation $\ln(\lambda/T)<-\ln n_{Si}$, where n_{Si} is the RI of silicon. Consequently, surface roughness at each interface can be modeled by a thin layer of thickness 2σ and of intermediate RI between air and silicon.[14] Including this virtual layer in the transfer matrix simulations, we found that the effect on the transmission spectrum was negligible. Therefore, with our fabrication process, surface roughness is not a limiting factor for optical multilayer applications. The variations between simulated and experimental results in Fig. 2 are most likely caused by imperfect parallelism between the optical planes. This imperfection, common to almost any DRIE process, was measured on SEM photographs of cleaved test structures and is smaller than 0.5°.

The simulated and experimental wavelengths at maximal transmission are plotted in Fig. 3 as a function of RI. As expected from the simulations (Fig. 2), the curve follows an essentially linear pattern with a sensitivity of 907 nm/RIU. The experimental results match the simulations perfectly, within the uncertainty on the RI of the liquids (±0.0005 RIU around $\lambda=1550$ nm).

As for the majority of RI sensors, the resolution of the RI measurement is limited by the uncertainty on the resonance wavelength measurement. Since our optical cavity has a relatively low quality factor ($Q=400$ for the $n=1.400$ resonance spectrum of Fig. 2), it is expected that the main source of uncertainty will be the amplitude noise that is superimposed to the resonance spectrum.[7] To quantify this source of error, we recorded the transmission spectrum of the cavity, filled with the $n=1.400$ liquid, 20 times at 90 s intervals. To attenuate the effect of the noise, the wavelength at maximal transmission was determined by fitting a fourth order polynomial to the maximal half of the resonance peaks. The obtained values of resonance wavelength had a standard deviation of $\sigma=0.005$ nm, which yields a detection limit of $3\sigma=0.015$ nm. From this and from the sensitivity reported above, the resolution of our sensor is $\Delta n=1.7\times10^{-5}$.

This resolution is the highest reported for a volume RI sensor integrated with a microfluidic system. Compared to resonant optical microcavities performing evanescent wave sensing, the resolution is two order of magnitude higher than the one reached with 2D photonic crystals[15] and two orders of magnitude lower than the state of the art $\Delta n \sim 10^{-7}$ resolution reached with optical ring resonators.[16]

The sensor is also very robust. During characterization, no particular attention was paid to cleanliness (quick dip in acetone between each measurement, out of clean room environment) and the sensor still works perfectly. A possible explanation for this is that only one of the six interfaces of each Bragg reflector is in contact with the liquid. While this interface gets contaminated, the other five remain perfectly clean and the impact on the optical response is limited. This might be an important advantage compared to other Fabry–Pérot cavities for which the mirrors are made of a single metallic coating.[11] Fabry–Pérot refractometers made of fiber Bragg gratings[10,12] also have the same advantage but the spatial overlap between the resonant electromagnetic field and the liquid is poor. This lowers the sensitivity and the resolution of the device by two orders or magnitude ($\Delta n = 1.8 \times 10^{-3}$ for Ref. 10) compared to our sensor.

The most important applications expected for the sensor are single living cells characterization and integration to chip-based liquid chromatography (LC) systems. Single-cell characterization is often performed in microfluidic systems using integrated refractometers.[9,11–13] This field of research could benefit from the high resolution and the robustness of our sensor but also from the possibility to simultaneously fabricate several devices. Chip-based LC systems are often fabricated using processes similar to the ones used for our sensor (DRIE of high aspect ratio silicon channels and pillars[17]). The integration of our sensor to such separation systems would be simple and could allow the detection of compounds that cannot be detected by absorption or fluorescence measurements (i.e., alcohols, carbohydrates, polymers, fatty acids, etc.).

We reported a microfluidic Fabry–Pérot refractometer based on vertically etched silicon Bragg reflectors. The resolution ($\Delta n = 1.7 \times 10^{-5}$ RIU) is the highest reported for a volume RI sensor integrated with a microfluidic system. The sensor is also very robust and should be useful for applications such as single living cell characterization and chip based LC.

[1] S. Yun and J. Lee, J. Micromech. Microeng. **13**, 721 (2003).
[2] C. Barrios, V. Almeida, R. Panepucci, B. Schmidt, and M. Lipson, IEEE Photonics Technol. Lett. **16**, 506 (2004).
[3] B. Saadany, M. Malak, M. Kubota, F. Marty, Y. Mita, D. Khalil, and T. Bourouina, IEEE J. Sel. Top. Quantum Electron. **12**, 1480 (2006).
[4] A. Lipson and E. Yeatman, J. Microelectromech. Syst. **16**, 521 (2007).
[5] J. Masson, F. Koné, and Y.-A. Peter, Proc. SPIE **6717**, 671705 (2007).
[6] M. Pruessner, T. Stievater, and W. Rabinovich, Appl. Phys. Lett. **92**, 081101 (2008).
[7] I. White and X. Fan, Opt. Express **16**, 1020 (2008).
[8] A. Llobera, R. Wilke, and S. Büttgenbach, Lab Chip **4**, 24 (2004).
[9] X. Liang, A. Liu, C. Lim, T. Ayi, and P. Yap, Sens. Actuators, A **133**, 349 (2007).
[10] P. Domachuk, I. Littler, M. Cronin-Golomb, and B. Eggleton, Appl. Phys. Lett. **88**, 093513 (2006).
[11] W. Song, X. Zhang, A. Liu, C. Lim, P. Yap, and H. Hosseini, Appl. Phys. Lett. **89**, 203901 (2006).
[12] L. Chin, A. Liu, C. Lim, X. Zhang, J. Ng, J. Hao, and S. Takahashi, Appl. Phys. Lett. **91**, 243901 (2007).
[13] H. Shao, W. Wang, S. Lana, and K. Lear, IEEE Photonics Technol. Lett. **20**, 493 (2008).
[14] A. Tikhonravov, M. Trubetskov, A. Tikhonravov, and A. Duparre, Appl. Opt. **42**, 5140 (2003).
[15] E. Chow, A. Grot, L. Mirkarimi, M. Sigalas, and G. Girolami, Opt. Lett. **29**, 1093 (2004).
[16] I. White, H. Zhu, J. Suter, N. Hanumegowda, H. Oveys, M. Zourob, and X. Fan, IEEE Sens. J. **7**, 28 (2007).
[17] J. Eijkel, Lab Chip **7**, 815 (2007).